PHYSICS RESULTS OF THE UA1 COLLABORATION AT THE CERN PROTON–ANTIPROTON COLLIDER

UA1 Collaboration, CERN, Geneva, Switzerland

Aachen – Annecy (LAPP) – Birmingham – CERN – Harvard – Helsinki – Kiel – Queen Mary College, London – NIKHEF, Amsterdam – Paris (Coll. de France) – Riverside – Rome – Rutherford Appleton Lab. – Saclay (CEN) – Vienna – Wisconsin Collaboration

(Presented by C. Rubbia)

1. INTRODUCTION

In this presentation I will summarize new physics results of the last year from the UA1 experiment at CERN. These data are from proton–antiproton collisions at a total centre-of-mass energy of 540 GeV, corresponding to an integrated luminosity of 136 nb^{-1}. The data were recorded mostly in the spring of 1983.

This paper is divided into two main sections. The first part deals with the observation of events with large missing transverse energy containing either a) a single electromagnetic cluster or b) a single jet. The second section is concerned with the search for the top quark.

2. EVENTS WITH MISSING ENERGY

In the absence of any non-interacting particles (e.g. neutrinos) and in the case of an ideal detector, we would observe perfect energy and momentum balance in each event. In practice, of course, we do not achieve this, but we can measure the transverse components fairly well. The longitudinal component of momentum balance cannot be measured with our detector because of energetic particles (typically 100 GeV) escaping down the beam pipe. Figure 1 shows how well the vertical component of transverse energy (E_T) is observed to balance for minimum bias events.[1] The missing E_T resolution for each transverse component may be parametrized as $\sigma = 0.43 \sqrt{\Sigma E_T}$, where ΣE_T is the scalar sum of transverse energies observed in the entire calorimeter. For events which contain high-transverse-momentum jets, the parametrization of the missing E_T resolution also holds. This is shown in Fig. 2, where we show the missing energy observed for a sample of two-jet events along with a Monte Carlo calculation of the expected distribution based on our parametrization of the resolution for each transverse component. For a typical event with

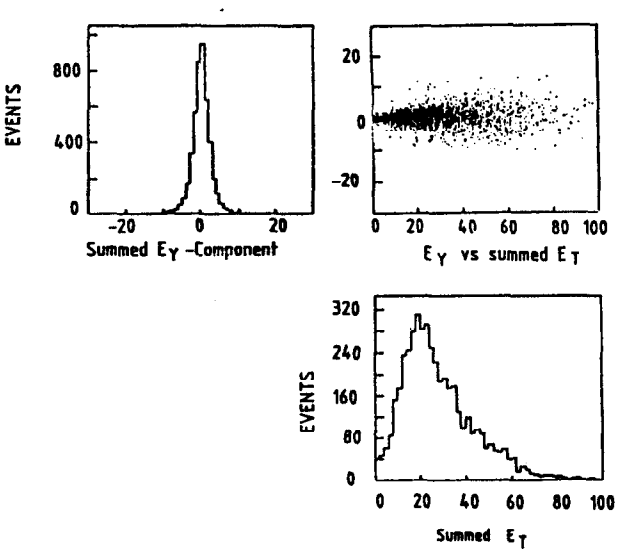

Fig. 1 : Scatter-plot of the vertical component of missing transverse energy versus the total transverse energy observed in all calorimeter cells.

ΣE_T = 80 GeV, we measure the missing transverse energy to about 6 GeV. To demonstrate a practical example, we show the missing transverse energy (ΔE_m) observed in a sample of identified $W \rightarrow e\nu$ decays (Fig. 3).[2] We find a sharp Jacobian peak at about one-half of the W mass.

The selection of events with large ΔE_m is given in Ref. [3]. We have looked in detail at all events having ΔE_m more than 4 st. dev. from zero. After vetoing such garbage events as beam halo and cosmic rays, we find 77 events passing the final selection. Figure 4a shows a plot of $(\Delta E_m)^2$ versus ΣE_T for these events: we find that 50 of them are part of the original $W \rightarrow e\nu$ sample; 27 are new. The new events are shown in Fig. 4b. We have classified them as having a single electromagnetic cluster, a single jet (with $E_T > 12$ GeV), two jets, or three or more jets.

Two events (G and H of Fig. 4b) have a single electromagnetic cluster without associated hard tracks. We have performed an inclusive 'photon' search by selecting all events with an isolated

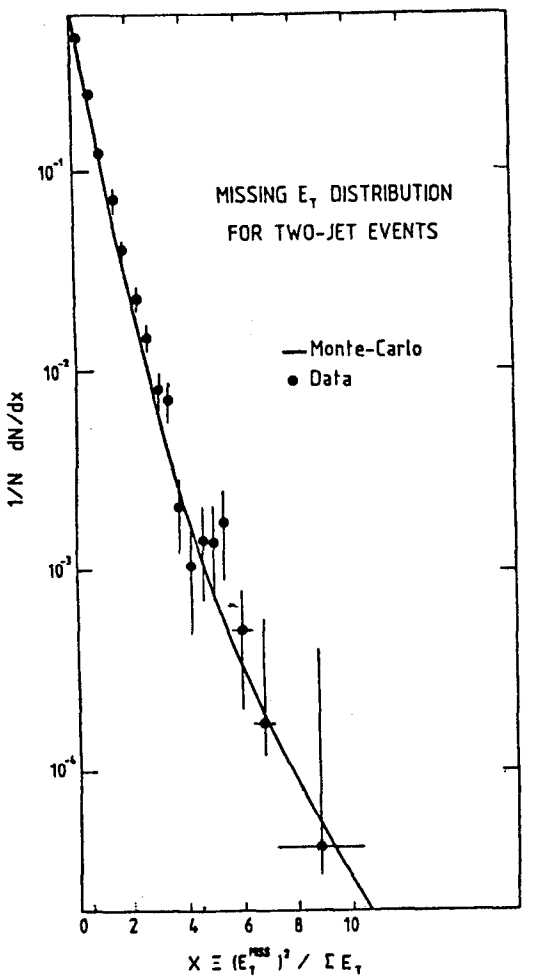

Fig. 2 : Transverse energy balance observed for a sample of two-jet events. To convert the horizontal scale to number of standard deviations (n), use the relationship $n^2 \approx 2x$.

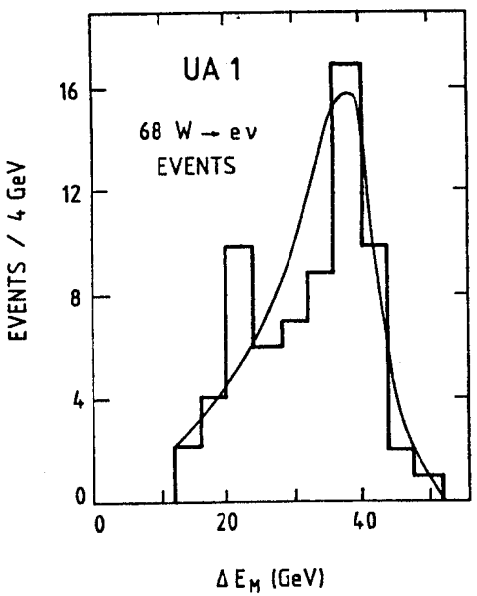

Fig. 3 : Missing transverse energy in $W \rightarrow e\nu$ events. The curve is the expectation for a W mass of 81 GeV, including our expected resolution.

electromagnetic cluster without a missing E_T requirement. This result is shown in Fig. 5 where we plot the 'photon' transverse energy against the missing E_T^2 of the event. The events with low missing E_T are consistent with QCD expectations of direct photon production and jet–jet events, where one of the jets fragments as one or more leading π^0's. However, events G and H have missing transverse energy far in excess of the other events. Events G and H represent a relatively large effect (about 10%) in the photon spectrum above 40 GeV E_T.

We have checked that the events G and H have clean interaction vertices and that the electromagnetic showers point to the vertex. We have also carefully checked to see if a charged track could have been missed in the central tracking chambers; this would be a potential background from $W \rightarrow e\nu$ decays. For event G we find that it is possible to have not detected a track (not even a single hit was observed) because the shower points within resolution to a small insensitive gap between the chambers.[1,3] For event H this is not possible because the shower

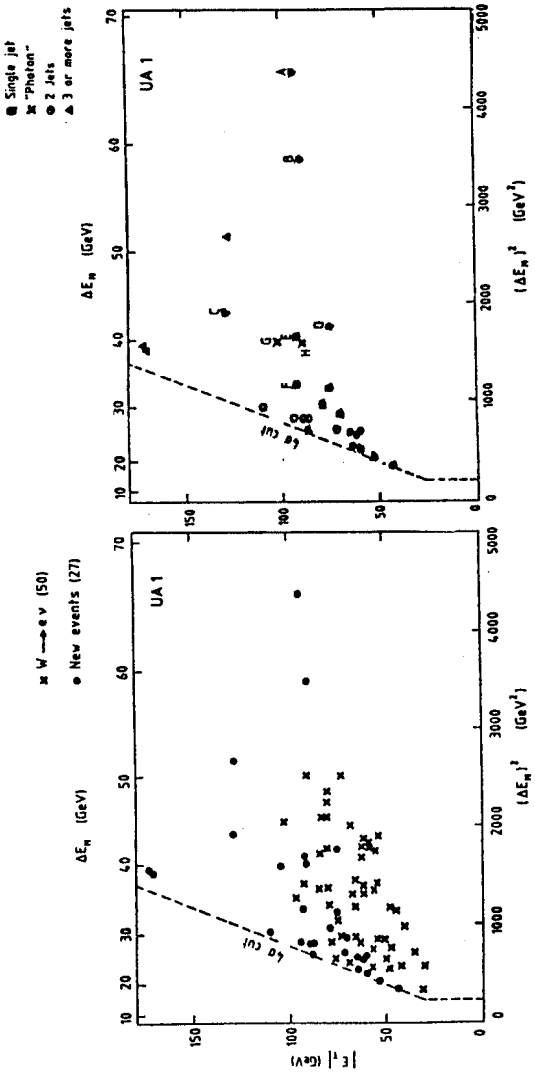

Fig. 4 : Missing transverse energy squared versus ΣE_T for all verified events which have ΔE_m more than 4 st. dev. from zero for a) all events and b) events with $W \rightarrow e\nu$ decays removed. The events are labelled according to their topology.

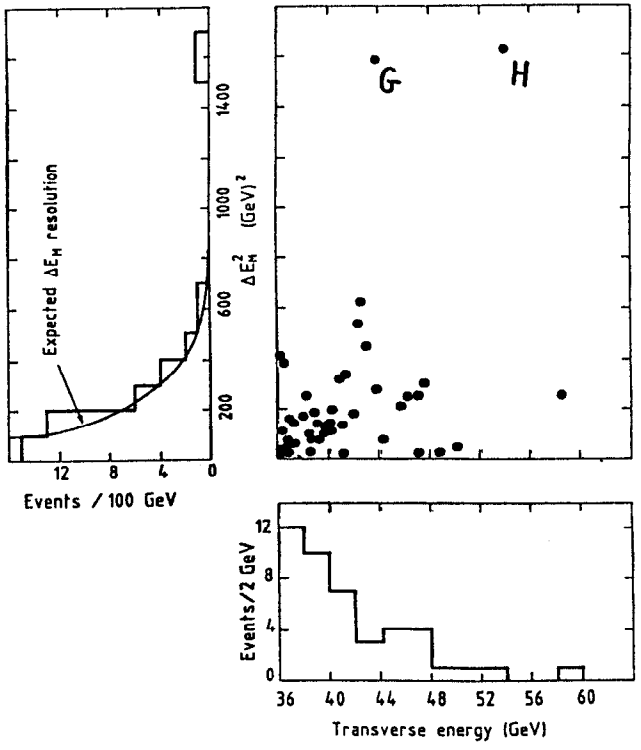

Fig. 5 : Transverse energy of the 'photon' candidate (note suppressed zero) plotted against the missing E_T of the event for the photon selection without a missing E_T cut. The solid curve is the expected missing E_T resolution for balanced events.

points to an active region of the chamber where we would expect about 20 hits and none were observed.[3]

Figure 6 shows the transverse energy flow for event H. The dominating structure in the event is a single electromagnetic cluster. The shower E_T is 54 GeV.

We find very low backgrounds for the 'photon' events. 'Photon' in this context means any number of nearly collinear photons of low (a few GeV) invariant mass. We have considered the following background possibilities:

i) $W \rightarrow e\nu$ where the electron track escapes detection.
This is possible for event G as explained previously, although its shower E_T of 44 GeV is somewhat higher than the average electron shower from W decay. For event H we could have a hard π^0 hit in the same shower counter as an electron from W decay, thereby shifting the observed shower position away from the blind region of the central detector. We can measure this background by looking at the π^0 rate in W events, and we find this background to be less than 0.002 events.

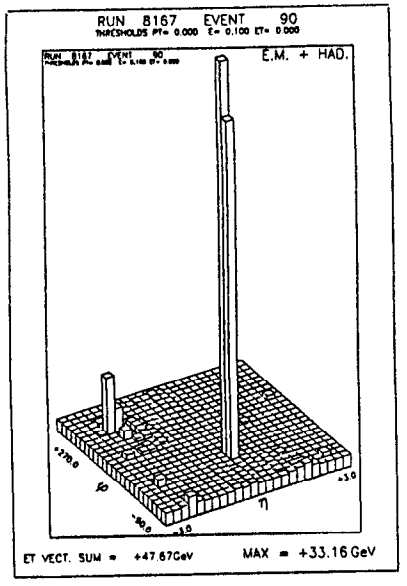

Fig. 6 : Transverse energy of the 'photon' candidate (note suppressed zero) plotted against the missing E_T of the event for the photon selection without a missing E_T cut. The solid curve is the expected missing E_T resolution for balanced events.

ii) Cosmic rays. Cosmic rays (in coincidence with a proton-antiproton soft collision) may shower in the lead/scintillator counters and fake a photon event. However, in general they do not point to the event vertex. This background is measured to be about 0.001 events.

iii) Fake shower response. Multiple π^0's may strike the same shower counter (e.g. one up and one down) and thereby appear as a single shower with missing E_T. This background is measured to be less than 0.007 events.

iv) Jet-jet fluctuations. An ordinary QCD two-jet event may fluctate in our calorimeter, so that one jet appears very soft and the other jet fragments into leading π^0's. This background is less than 0.001 events.

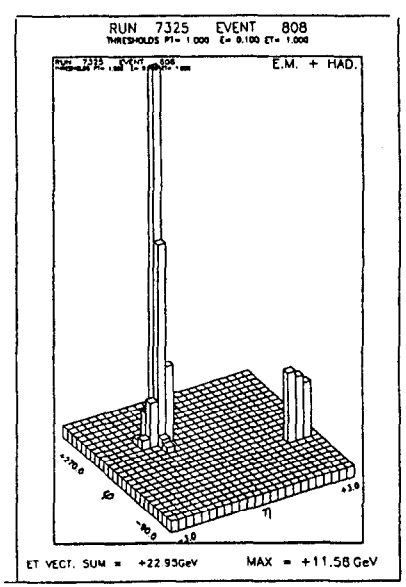

Fig. 7 : Transverse energy flow observed in the calorimeters for monojet event A. There is in addition an energetic muon in the jet.

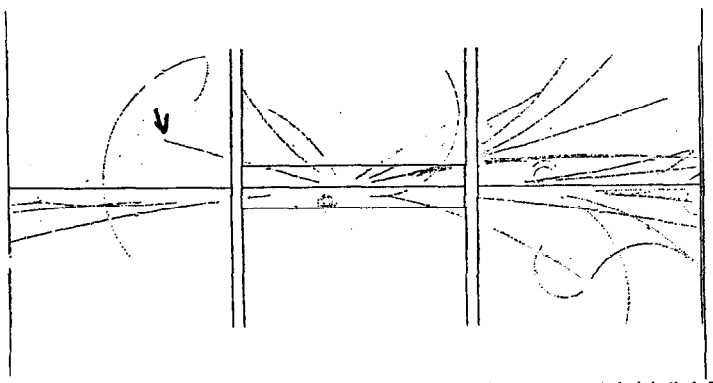

Fig. 8 : Central detector digitization display for event A. The muon track is labelled. The event has a clear interaction vertex and relatively low multiplicity (about 20 charged tracks).

We now turn to a description of the single-jet events of Fig. 4b, which have the largest missing transverse energy. Event A is a remarkable event. The transverse energy flow observed in the calorimeters is shown in Fig. 7. In addition there is an energetic muon within the jet which makes an angle of about 100 mrad with the calorimeter cluster. There are no other charged tracks in the jet (see Fig. 8). The momentum of the muon is measured independently in the central detector ($p = 80^{+20}_{-13}$ GeV/c) and the muon system ($p = 105^{+59}_{-27}$ GeV/c). [4] The missing E_T in the event is 66 GeV.

The transverse energy flow in event B is shown in Fig. 9. A single jet (E_T = 48 GeV) dominates the event structure. The missing energy of this event is 59 GeV. An event display is shown in Fig. 10.

To help determine the background from two-jet fluctuations, we have relaxed the cut on ΔE_m from 4 st. dev. to 2 st. dev. We have also applied a cut on $\Delta\phi$, the angle in the transverse plane that the rest of the event (jet not included) makes with respect to the jet. This is shown in Fig. 11. Events A-F, which all pass the $\Delta\phi$ cut, exceed the background expected from jet fluctuations (e.g. a two-jet event where one jet is observed to be very small).

For the monojet events A-F with $\Delta E_m > 30$ GeV we have considered the following backgrounds:

i) $W \rightarrow \tau\nu$. We expect about two events with the missing E_T distribution shown in Fig. 11. Only event F, by nature of its lower jet E_T, low jet mass, and three-prong multiplicity, is consistent with this process.

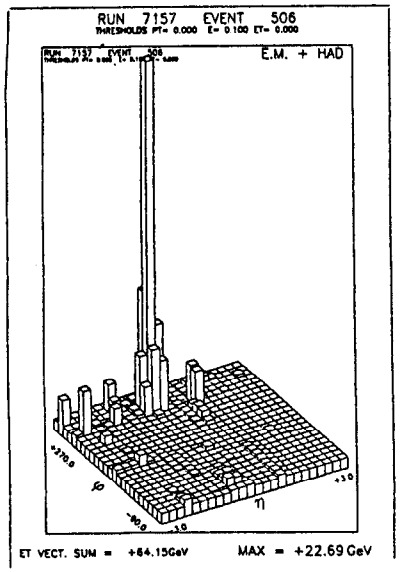

Fig. 9 : Transverse energy flow for monojet event B. The jet E_T is 48 GeV.

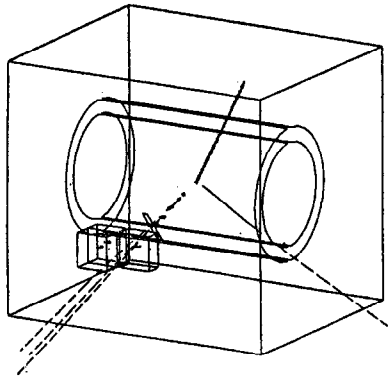

Fig. 10 : Event display showing tracks with $p_T > 2$ GeV/c and calorimeter hits with $E_T > 5$ GeV. The arrow indicates the direction of the missing E_T (59 GeV).

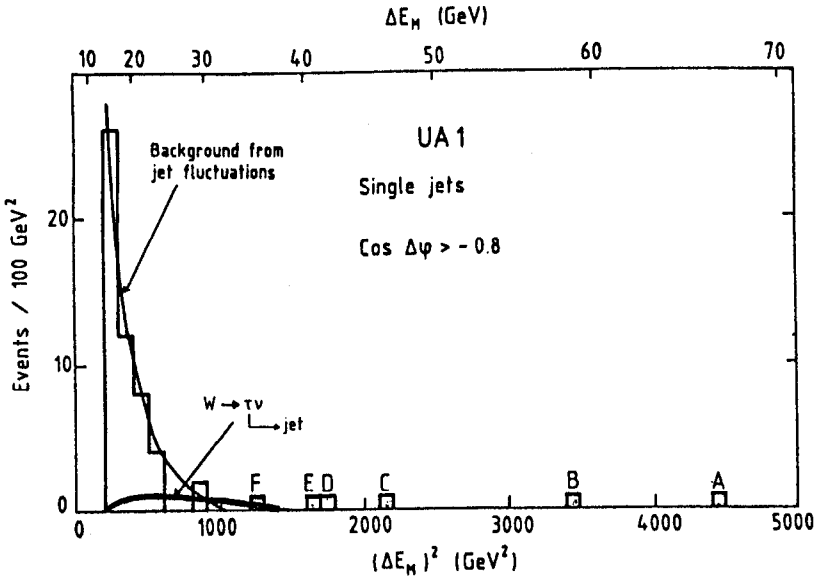

Fig. 11 : Distribution of missing E_T^2 for events passing the 2σ cut on missing E_T and the cut $\cos\Delta\gamma < 0.8$.

ii) $W \to L\nu$, where L is a new sequential heavy lepton. The background for any heavy lepton is smaller than that for the τ owing to phase space and decay kinematics.

iii) gZ^0. A gluon-jet could be produced in association with a Z^0 which could then decay into $\nu\bar{\nu}$ (expected branching ratio is nearly 20%). However, no jets are observed in W or Z^0 events with $E_T > 25$ GeV.

iv) c, b, t quark decay. We could have heavy quark pairs with one of them decaying into a leading neutrino. We expect less than 0.1 events from this process. A direct search for lepton-jet events with an electron or muon and a jet E_T greater than 30 GeV gives no events.

We find no two-jet events (Fig. 4b) to be in excess of expected backgrounds. We find one three-jet event (the one with the largest ΔE_m in Fig. 4b) to be far in excess of the background from jet fluctuations. The jets have E_T's of about 55 GeV, 20 GeV, and 15 GeV, and the event has a missing E_T of about 55 GeV.

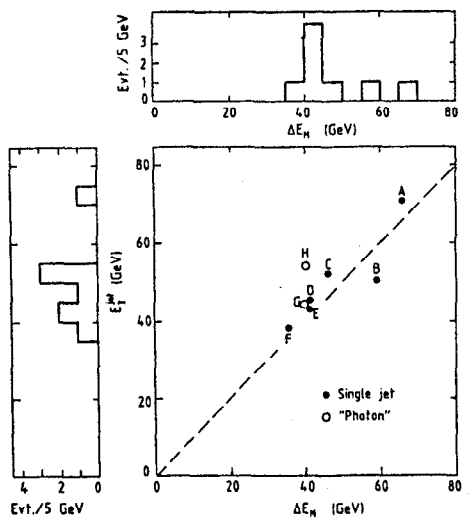

Fig. 12 : Missing transverse energy versus cluster E_T for events A–H.

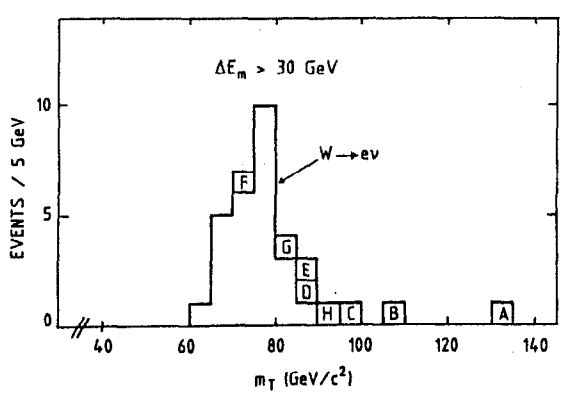

Fig. 13 : Transverse mass distribution.

A plot of the missing E_T against jet E_T is shown in Fig. 12 for events A–H. A clustering near the dashed line (ΔE_m = E_T jet) indicates that the observed missing E_T is mainly due to a single unbalanced cluster.

Figure 13 shows a plot of transverse mass of the jet and missing E_T for events A–H, plus the three-jet event along with a sample of W events with missing E_T greater then 30 GeV. The observed mass distribution of events A–H exceeds that of the W→ eν decays.

The interpretation of these missing E_T events awaits the accumulation of more data. One possibility is that the missing energy is due to some new particle, e.g. the photino ($\tilde{\gamma}$) of supersymmetric theories. These data would then place some constraints on the masses of the supersymmetric particles.[4] Another natural source of missing energy is from the Z^0 decaying into neutrinos. Under the hypothesis that a high-mass state X decays into Z^0 + jet, we may calculate the mass range of X allowed for each event from energy and momentum conservation. This is shown in Fig. 14. The data do not rule out such a process for the mass of X of about 170 GeV.

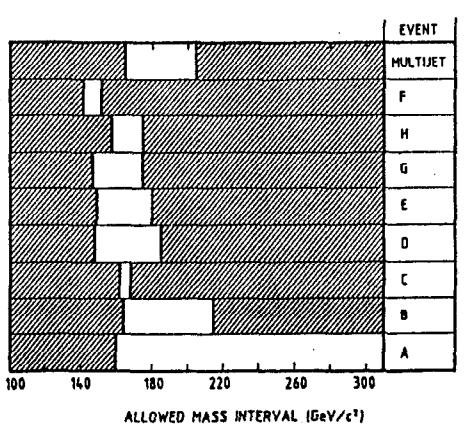

Fig. 14 : Allowed mass range for hypothetical particle X which decays into Z^0 + jet, with the Z^0 decaying into neutrinos. A common mass of about 170 GeV is not ruled out.

Finally, we remark that if these events were due to the production and decay of a new massive state, we might hope to see structure in the two- or three-jet mass spectrum. No such structure is observed within our present statistics and mass resolution. The two-jet spectrum is shown in Fig. 15.

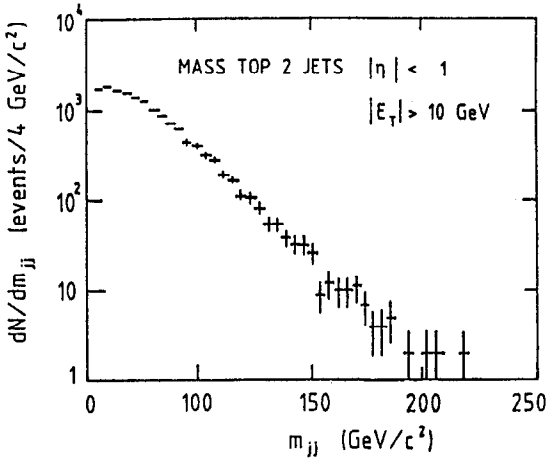

Fig. 15 : Observed two-jet mass spectrum (not corrected for acceptances). No significant structure is observed.

3. SEARCHING FOR THE TOP QUARK

The UA1 Collaboration has recorded 68 events with $e^{\pm}\nu_e$ decays [5] of the charged Intermediate Vector Boson (IVB), and a more restrictive sample of $W^{\pm} \to \mu^{\pm}\nu_\mu$ decays [6] (14 events). These events have a remarkably clean signature: the main kinematical effect of the composite nature of the initial hadrons is limited to a longitudinal motion and a transverse kick to the IVB. Occasionally, the emission of one or more QCD jets radiated from the incident quark legs is also observed.[7] In agreement with expectations for initial state bremsstrahlung, these jets are emitted primarily along the incoming beam directions and have a rapidly falling transverse energy distribution.

Observation of the electronic and muonic decay modes of the IVB has provided an understanding of the production process and has built up confidence in the apparatus necessary to extend the search to the quark decay modes. The structure of the weak current responsible for the hadronic decays of the IVB's is expected to be coupled to charge 2/3 quarks and to the Cabibbo-rotated states d_c, s_c, b_c (namely, linear combinations of charge 1/3 quarks) with the same strength as the coupling to leptons. From the number of observed leptonic decays, taking into account detection efficiencies and colour factors, we conclude that (255 ± 30) $W^{\pm} \to ud_c$ and the same number of $W^{\pm} \to cs_c$ must also have been produced in the same run. Unfortunately, the observation of these decays is made very difficult by the presence of a relatively large QCD jet background.

The present paper deals with the search for the sixth quark, the t-quark (top or truth), which completes the family of the weak currents with a third doublet ($t\bar{b}_c$) which manifests itself in the decay $W^+ \to t\bar{b}_c$ (and also $W^- \to \bar{t}b_c$), provided $m_t < m_W - m_b$. Previous, unsuccessful searches for the t-quark in e^+e^- colliding beams [8] have established a mass limit $m_t \geq 22$ GeV/c². Using the available energy in the decay $W^{\pm} \to tb_c$, we can extend the search up to masses of about 65 GeV/c², since the t-quark is produced in association with relatively light quarks. For $m_t = 40$ GeV/c² the reduction factor with respect to massless quarks is 0.71, giving, before detection cuts, an expectation of (181 ± 20) $W^{\pm} \to tb_c$ decays from our integrated luminosity.

We concentrate on the semileptonic decay channel of the t-quark:

$$W^+ \to t\bar{b}_c (t \to \ell^+ \nu b_c) \qquad \ell \equiv \text{(electron, muon)}$$

(and the corresponding reaction for W^-). In spite of the smaller number of events due to the additional leptonic branching ratio, this channel is chosen for the clean signature it provides, i.e. two jets, a lepton, and some missing transverse energy ($\not{\nu}$).[9] These events have several features which permit them to be identified and separated from other sources of background:

i) The invariant mass of the $(b_c\bar{b}_c\ell\nu)$ system must peak around the W mass. Replacing the neutrino momentum $\vec{p}_\nu$ by the measured missing transverse energy $\Delta\vec{E}_m$ [9] broadens the peak somewhat, with a small shift of the average mass value.

ii) The invariant mass of the $(b_c\ell\nu)$ system must be compatible with a common value, namely m_t [10] (to a good approximation after the substitution $\vec{p}_\nu \to \Delta\vec{E}_m$).

iii) The t-quark is heavy ($m_t \geq 22$ GeV/c²) and therefore relatively slow in the laboratory. Angles between particles from the decay in the laboratory are very wide. Furthermore, the lepton momentum has a major component normal to the b_c jet, p_n. In the case of decays of lighter quarks (b,c), $p_n \lesssim (m_b/2, m_c/2)$.

iv) The recoiling $\bar{b}_c$ jet has a characteristic Jacobian peak in the transverse energy distribution, which makes it possible, in most cases, to distinguish it from the other, lower-energy b_c jet.

As discussed in detail further on, a simple set of topological cuts on the event configuration enables us to extract an essentially background-free event sample. However, the number of surviving events is also considerably reduced. For a semileptonic branching ratio ~ 1/9 ('naive'

prediction based on lepton and quark counting) and $m_t = 40$ GeV/c^2, we expect (20 ± 2.2) electrons (both signs) and an equal number of muons. With reasonable cuts on the transverse energy of jets and leptons [$E_T(\bar{b}_c) > 8$ GeV; $E_T(b_c) > 7$ GeV; $p_T(\ell) > 12$ GeV/c] we arrive at (4 ± 0.3) events for each leptonic channel, before geometrical and track isolation cuts.

Searching for this small number of events deserves some remarks:

i) Both the muon and the electron samples will be used in order to increase the significance of the result. Evidence of an effect must rely on its independent observation in *both* decay channels.

ii) The electron and muon identification must be considerably improved with respect to the previous search for leptonic IVB decays, since now the signal is only ~ 1/20 of the $W \to \ell + \nu$ rate and the average lepton energy is a factor of ~ 3 smaller, which greatly enhances the probability of hadrons simulating the leptonic signature. Furthermore, the event topology requires a dominant jet activity, thus enhancing QCD associated backgrounds.

Finally, a residual leptonic signal due to $W \to t\bar{b}_c$ decays must be clearly separated from production of ($b\bar{b}$) and ($c\bar{c}$) with subsequent associated semileptonic decays, which are copious sources of leptons and jets. The cross-section and kinematics of heavy quark pair-production via gluon-related and quark-related strong interaction graphs are relatively poorly known at collider energies. In order to extract from the data the information needed to reliably evaluate the expected background from this source, a parallel experiment has been performed aimed at strong interaction production of heavy quarks.

3.1. The electron sample

As described extensively in previous publications [1,11] to which we refer the reader for details, after momentum (p) determination from the magnetic curvature measured by the central detector, electron identification is based on absorption in the 27 X_0 of a 4π lead/scintillator calorimeter hodoscope segmented four times in depth (3 X_0, 7 X_0, 10 X_0, 7 X_0), followed by a hadron calorimeter in which only a small residual energy E_{had} is expected. Each of the four segments of the lead/scintillator calorimeter cells is read out by four independent photomultipliers in a way that permits the determination, by pulse division, of the centroid of the energy deposition in two orthogonal directions.

In the previously reported observation of the $W^\pm \to e^\pm \nu_e$ decay,[5] very generous selection criteria were sufficient to obtain an essentially pure event sample, namely: i) a charged track of $p_T > 7$ GeV, of projected length > 30 cm and with at least 20 digitizings; ii) an energy deposition of $E_T > 15$ GeV in two adjacent e.m. cells; iii) a match within 5 st. dev. between the impact of the track and the centroid of the energy depositions in the calorimeter; iv) an energy deposition $E_{had} <$ 600 MeV in the subsequent hadronic calorimeter; v) electron isolation, namely no more than 10% of the electron energy is allowed for any additional energy deposited in a cone around the electron track $\Delta R \equiv (\Delta\eta^2 + \Delta\phi^2) \leq 0.7$, where ϕ is the azimuthal angle measured in degrees and η is the rapidity; and vi) no jet back-to-back in ϕ with respect to the electron within ±30°. In this way, we have detected 49 $W^\pm \to e^\pm \nu_e$ decays, completely background free and satisfying the additional condition [9] $\Delta E_m > 15$ GeV. These events give us an ideal electron calibration sample for the present search.

However, as soon as the limitation on the jet activity (vi) and the missing-energy requirements are dropped, we find a much larger sample of presumably heavily contaminated events. Requiring the electron transverse energy $E_T > 12$ GeV, and tightening the E_{had} condition to $E_{had} < 200$ MeV leaves us with as many as 152 events. A first reduction of the sample can be achieved by removing π^0 conversions in the beam tube and in the walls of the central detector. These events can easily be recognized, by scanning or program, by looking for tracks which have a small minimum distance D from the electron track. As one can see from Figs.16a and 16b, there is a large peak centred around D = 0, mostly from track pairs having charges of opposite signs. Applying a cut on D at 3σ, forty-three conversions are removed. Recognition of conversions by program and by scanning agree very well, and the number of conversion events is in agreement with expectations,[12] based on the flux of high-energy π^0's and the amount of material traversed.

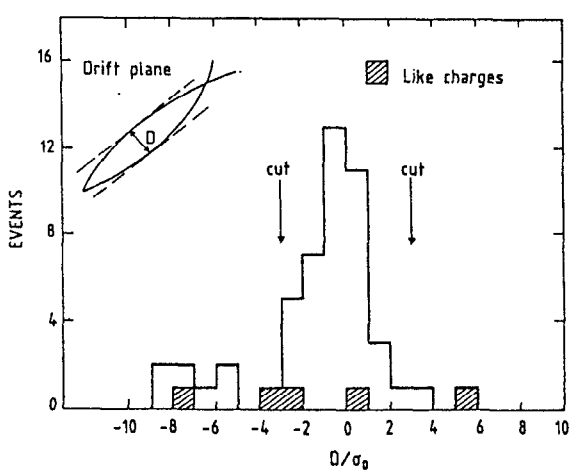

Fig. 16 : Identification of π^0 conversions. a) The minimum distance D between the energetic electron candidate and the nearest track in the drift plane of the central detector is shown normalized by the error on this quantity. When the unreconstructed partners recognized by visual scanning are included, a cut at 3σ removes 43 conversions.

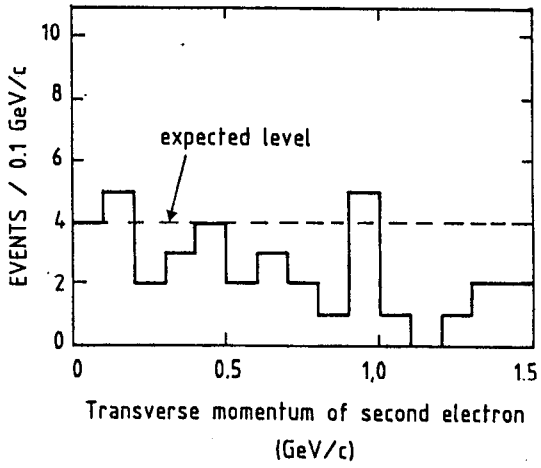

Fig. 16 : b) The rate of identified conversions shown as a function of the transverse momentum of the low-p_T partner, compared with the expected rate.[12] The small loss at higher values of p_T reflects the isolation criteria imposed on the energetic electron.

The remaining 109 events are still largely contaminated by multiple particle overlaps, namely jets with one charged energetic hadron and one or several π^0s simulating the e.m. behaviour. In order to eliminate this background, we raise the electron transverse energy threshold to 15 GeV and make use of the full rejection power of the detector, namely: i) a good match between the momentum measurement and the energy deposition in the calorimeters, $|(1/p) - (1/E)| < 3\sigma$; ii) a good electromagnetic shape in the energy depositions of the four e.m. segments, characterized [13] by $\chi^2_R < 20$; and iii) a stricter isolation requirement for the electron track, namely that the Σp_T of all other tracks and the energy deposited in all calorimeters ΣE_T be less than 1 GeV in a cone of $\Delta R \leq 0.4$ around the track. This new selection leads to twelve events, namely seven events with electrons and one jet and five events with at least two jets. Forty-four out of the forty-nine W events survive these cuts. One can compare the distributions of ΣE_T versus χ^2_R for the calibration sample of $W^\pm \to e^\pm \nu_e$ decays (Fig. 17a), the sample of single jets (Fig. 17b), and the sample of events with at least two jets (Fig. 17c). Whilst both the ≥ 2 jet events and $W \to e^\pm \nu_e$ events have a cleanly isolated electron and small values of χ^2_R, the single-jet events are more widely distributed, and indeed their precise number depends on the choice of our cuts, indicating that in general they are not truly isolated. We concentrate on the five events with ≥ 2 jets. Their main parameters are listed in Table I. Their

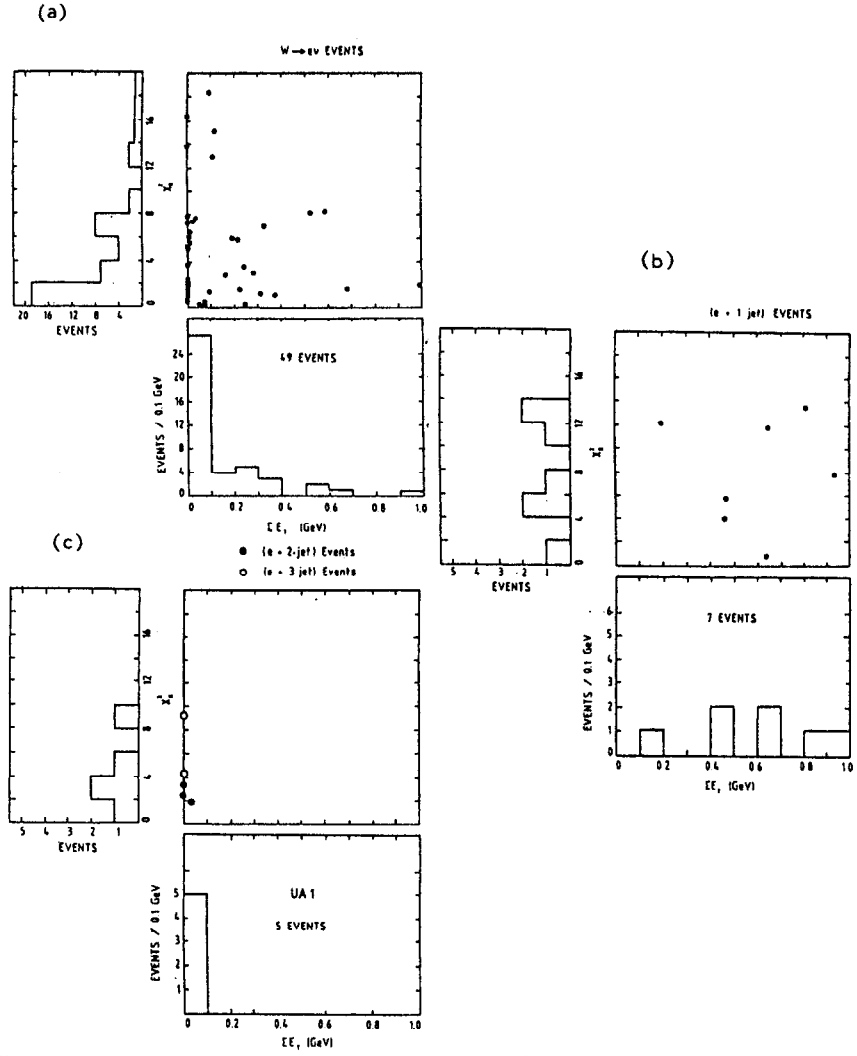

Fig. 17 : Electron isolation. The electron quality parameter χ^2_R [13] is shown as a function of the energy accompanying the electron candidate in a cone of $\Delta R \leq 0.4$ around the track. This is shown for a) $W \to e^\pm \nu_e$ events, b) $e^\pm$ + single jet events, and c) $e^\pm + \geq 2$ jet events.

Table 1

Event parameters for the isolated electron + 2 jet events

Event	Electron				ΔE_{in}	Jet 1			Jet 2				$m(e\gamma_T' j_1 j_2)$	$m(e\gamma j_1 j_2)$
	Q	E_T (GeV)	η	ϕ (deg.)	(GeV)	E_T (GeV)	ϕ (deg.)	η	E_T (GeV)	ϕ (deg.)	η	$\cos\theta^*$	(GeV/c^2)	(GeV/c^2)
6301/716	+	19.5 ± 0.8	−0.6	−114	6.7 ± 5.6	14.0	29	0.1	13.9	153	−0.3	−0.06	61 ± 5	40 ± 4
7443/509	−	19.1 ± 0.7	1.2	12	4.5 ± 6.4	23.4	134	0.2	11.1	−114	−0.7	−0.73	76 ± 7	48 ± 7
8578/983	−	18.3 ± 0.7	−1.1	132	5.1 ± 6.4	22.6	−19	0.5	15.5	−145	−0.2	0.02	82 ± 7	42 ± 5

electron properties closely resemble the ones of the W calibration sample (Fig.18). Next we shall evaluate the expected background.

As already pointed out, the dominant background is expected to come from QCD jets faking electrons by fragmenting, such that one energetic charged pion overlaps with one or more neutral pions. Two methods have been used to estimate this background: i) a global method, using a π^0 + $\geq$ 2 jet data sample, in which the shape of the expected QCD background distribution is compared with the shape of the corresponding distributions for the candidate events; and ii) a direct method in which the absolute rate of $(\pi^{\pm}+n\pi^0)$ + jet events is extracted a the $\pi^{\pm}$ + jet selection. The probability that the selected $\pi^{\pm}$ pass the isolated electron selection criteria is then folded into the resulting estimated background rate.

The shape of the QCD background from π^0 + $\geq$2 jet events is shown in Fig.19a, in which the transverse energy component of the isolated π^0 perpendicular to the plane formed by the $p\bar{p}$ axis and the highest E_T jet (j_1) is plotted as a function of $\cos\theta^*_{j_2}$. The angle $\theta^*_{j_2}$ is between the average ($p\bar{p}$) beam axis and the lowest E_T jet (j_2) in the ($\pi^0 j_1 j_2$) rest frame. The five electron + $\geq$2 jet events (Fig. 19b) are all contained within a region RI = ($E_T^{out} > 8$ GeV, $|\cos\theta^*_{j_2}| < 0.7$), whilst the majority of background QCD events lie in the complementary region RII.[14]. Table 2 summarizes

Table 2

The number of events in the two regions of the E_T^{out} versus $\cos\theta^*_{j_2}$ plane (see text)

Region	π^0	e
π^0/electron + $\geq$2 jets (RI + RII)	933	5
RI = ($E_T^{out} > 8$ GeV, $\|\cos\theta^*_{j_2}\| < 0.7$)	211	5
RII = I − RI	722	0

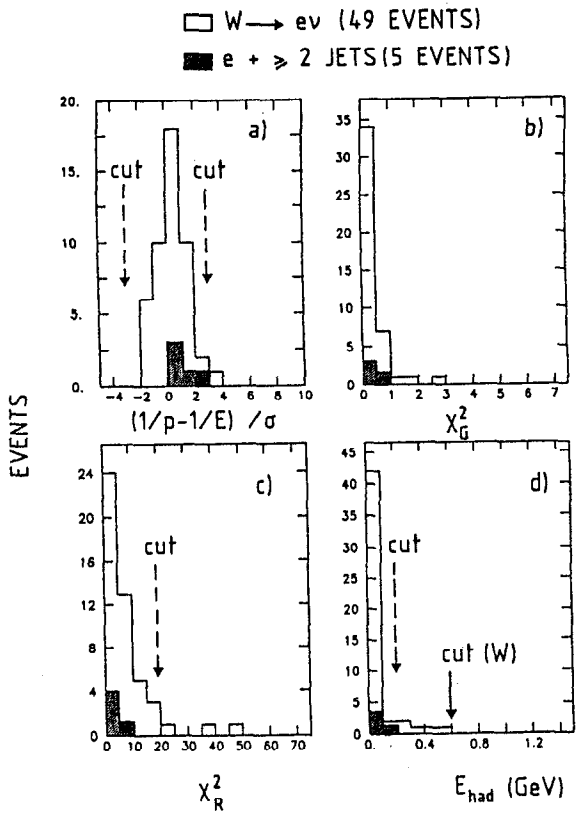

Fig. 18 : Electron quality. The quality of the electrons in the e + $\geq$2 jet sample (shaded) is compared with the control sample of electrons from $W^{\pm} \rightarrow e^{\pm}\nu_e$ decays. The quality variables shown are: a) the matching between the momentum measurement and the calorimeter energy deposition; b) the quality of the matching between the track direction measured in the central detector and the direction measured by pulse division in each of the four segments of the e.m. calorimeter; c) an over-all quality parameter χ^2_R [13] measuring the electromagnetic shape of the longitudinal shower profile and the pulse sharing between the different calorimeter samples; and d) the energy deposited in the hadron calorimeter behind the electromagnetic shower.

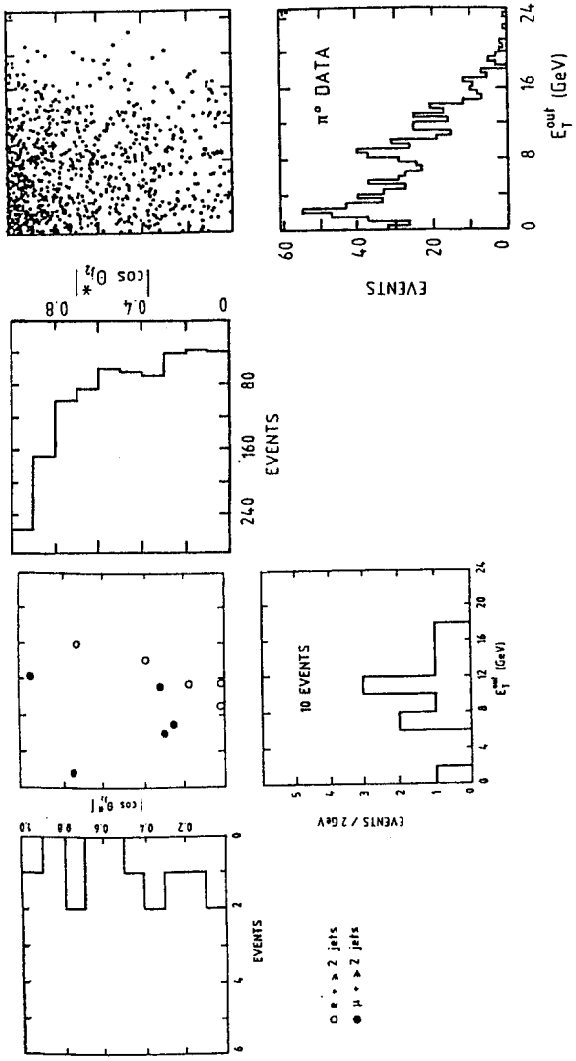

Fig. 19 : a) Expected shape of the QCD background extracted from $\pi^0 + \geq 2$ jet events. The transverse energy component of the isolated π^0 perpendicular to the plane formed by the $p\bar{p}$ axis and the highest-E_T jet, E_T^{out} is plotted as a function of $\cos\theta_{j_2}^*$. The angle $\theta_{j_2}^*$ is between the average beam axis in the three-body rest frame and the lowest-E_T jet (j_2). b) As above but for the isolated electron + ≥ 2 jet events (open circles) and the isolated muon + ≥ 2 jet events (full circles).

the number of events in these two regions. On the basis of these statistics the probability that the QCD background events have a distribution identical to the five electron + ≥2 jet events is 8×10^{-5}, i.e. a 4σ difference in shape. The choice of regions RI and RII, however, is arbitrary and a comparison of shape with the Kolomogorov test gives a probability of 5.2×10^{-4}, i.e. a 3.5σ difference.

To determine the absolute magnitude of the background from $\pi^{\pm} + \geq 2$ jet events, we estimate the probability that a $\pi^{\pm}$ satisfies the isolated electron selection criteria. Of the 169 $\pi^{\pm} + \geq 2$ jet events originally selected, 68 satisfy the electron trigger requirement of $E_T > 12$ GeV. The probability that these charged pions fake an isolated electron is estimated to be 1.5×10^{-3}, yielding a total of 0.1 background events.[15] Results of this background calculation are given in Table3a. The corresponding number of background events in region RI is less than 0.06.

Finally the background from unseen conversions with one electron triggered with $p_T >$ 15 GeV/c and the other electron unobserved ($p_T < 0.05$ GeV/c) is less than 0.02 events, determined from the measured π^0 flux in region RI. Therefore, we conclude that the five events with at least two jets have genuine electrons.

3.2 The muon sample

A simple set of cuts is used to arrive at a sample of isolated muons with one or more jets: i) a muon track in the central detector with $p_T^{(\mu)} > 12$ GeV, good geometrical match in the muon chambers, track projected length ≥ 40 cm, and at least 30 digitizings; ii) isolation, namely $\Sigma p_T < 0.1\ p_T^{(\mu)}$, $\Sigma E_T < 0.2\ p_T^{(\mu)}$, where the sum extends to all tracks and calorimeter hits in a cone $\Delta R \leq 0.4$. Forty events survive these cuts. The dominant source of background comes from the decays of pions and kaons in the central detector drift volume. In the case of slow kaons, parent and daughter tracks may form a kink in the track digitizings in a configuration which is reconstructed as a single fake high-momentum track. After visual scanning and rejection of obvious $K \rightarrow \mu\nu$ decays in flight within the central detector volume (kinks), and an enhanced isolation requirement of no jet within a distance $\Delta R \leq 1$ from the muon, we are left with twelve events, seven with one jet, four with two jets, and one with three jets. Again we concentrate on the ≥2 jet events, which are listed in Table 4. The residual decay background has been determined from a 5 nb^{-1} data sample collected with a low threshold ($E_T > 15$ GeV) jet trigger. This trigger requirement is satisfied by the five muon + ≥ 2 jet events. We wish to estimate the probability that decaying hadrons (π,K → $\mu\nu$) pass our track-quality cuts and are reconstructed with $p_T > 12$ GeV/c. The final background rate is then the convolution of this probability (per decaying hadron) with the measured p_T spectrum of the 5 nb^{-1} sample. For a mixture of 50% pions and 25% kaons, this probability is typically 2×10^{-3} for a hadron with a p_T of 13 GeV/c to be reconstructed with $p_T > 12$ GeV/c.

The results of this background calculation are summarized in Table 3b. We find that the corresponding number of decay muon + ≥ 2 jet events is 0.4, giving less than 0.10 background events for $|\cos\theta_{j_2}^*| < 0.8$. In Fig. 19 the E_T^{out} is plotted versus $\cos\theta_{j_2}^*$ for the five muon + ≥ 2 jet

Table 3a

Expected background to e + ≥ 1 jet events arising from charged pions faking an isolated electron with $E_T > 15$ GeV. Both the normal trigger data sample and a low threshold (5 nb^{-1}) trigger data sample give consistent results.

Event sample	Channel	Expected background	
		Isolated[a]	Super-isolated[b]
Normal trigger	$\pi^\pm$ + 1 jet	0.7 ± 0.2	0.3 ± 0.1
	$\pi^\pm$ + 2 jets	0.36 ± 0.14	0.10 ± 0.04
Low-threshold (5 nb^{-1})	$\pi^\pm$ + 1 jet	1.1 ± 0.3	0.65 ± 0.25
	$\pi^\pm$ + 2 jets	0.3 ± 0.2	0.06 ± 0.04

a) Isolation criteria in a cone $\Delta R \leq 0.4$: $\Sigma E_T < 1$ GeV, and $\Sigma p_T < 1$ GeV/c (see text).
b) Super-isolation criteria, demanding the additional isolation requirements in a cone $\Delta R \leq 0.7$; $\Sigma E_T < 2$ GeV, and $\Sigma p_T < 1.5$ GeV/c. The candidate e + ≥ 2 jet events satisfy these criteria.

Table 3b

Expected background to μ + ≥ 1 jet events arising from the decay of charged pions and kaons in the central detector volume. The low-threshold trigger (5 nb^{-1}) data sample has been used. There is a systematic uncertainty of a factor of 2 on the normalization of these estimates.

Cuts	Events	Background estimate	
		No isolation	Isolated[a]
$p_T^\mu > 12$ GeV/c; ≥ 1 jet with $E_T > 8$ GeV and $\lvert\eta\rvert < 2.5$	6	9.0	0.9
$\Delta R(\mu, \text{jet}) > 1$[b] ≥ 2 jets with $E_T > 7$ GeV and $\lvert\eta\rvert < 2.5$	4	3.8	0.4
Exactly 2 jets with $E_T > 7$ GeV	3	2.4	0.2
$\lvert\cos\theta^*_{j_2}\rvert < 0.8$	3	1.5	0.1

a) Isolation in a cone $\Delta R \leq 0.4$.
b) Distance ΔR between μ and nearest jet with $E_T > 7$ GeV.

Table 4

Event parameters for the isolated muon + 2 jet events

Event	Muon				ΔE_m	Jet 1			Jet 2				$m(\nu_T j_1 j_2)$	$m(\nu_T j_2)$
	Q	p_T (GeV)	η	ϕ (deg.)	(GeV)	E_T (GeV)	ϕ (deg.)	η	E_T (GeV)	ϕ (deg.)	η	$\cos\theta^*$	(GeV/c^2)	(GeV/c^2)
6639/118	+	16.0 ± 3.4	0.9	103	5.3 ± 7.0	30.0	−70	−0.4	11.1	23	−1.0	−0.76	79^{-7}_{+10}	41^{-6}_{+11}
7501/117	−	13.5 ± 1.0	−0.3	112	7.5 ± 7.0	22.9	−41	−0.8	20.2	−179	−1.0	−0.30	75 ± 7	43 ± 9
7935/232	−	16.2 ± 3.3	0.4	65	$5.8^{+7.0}_{-6.0}$	25.1	−140	1.7	11.3	−13	1.0	−0.25	78^{-4}_{+5}	37 ± 9

events, the e/π^0 + ≥ 2 jet events. Of the four muon + 2 jet events, one event is most likely a background event of QCD origin since the lowest E_T jet j_2 lies close to the beam axis with $\cos\theta^*_{j_2} = 0.93$. This event has been removed from the data sample.

3.3 Backgrounds due to beauty and charm pair production

Events with the topology of two jets and an isolated large-p_T lepton can be produced at some level by more conventional processes not containing a t-quark. Of particular relevance is the case in which the prompt lepton is produced by the semileptonic decay of a large-p_T b-quark or a c-quark. These events ordinarily appear as two jets back-to-back in azimuth with the lepton embedded in one of the two jets and therefore they will not meet our isolation requirements. However, they can simulate the topology of our events provided the lepton is the leading particle (thus suppressing the isolation veto) and another central jet is produced by second-order QCD processes, namely

$$\begin{aligned} gg &\to gb\bar{b}(gc\bar{c}), \\ q\bar{q} &\to gb\bar{b}(gc\bar{c}), \\ qg &\to qb\bar{b}(qc\bar{c}). \end{aligned} \qquad (1)$$

Since the heavy quark cross-sections are expected to be much larger than the $W \to t\bar{b}$ rate, these backgrounds deserve a careful analysis. So far, QCD predictions for heavy-flavour production of large p_T at the Collider have not been verified by experiment. To this purpose we have selected *inclusively* all events in which a muon of $p_T > 12$ GeV/c is accompanied by at least one jet of transverse energy $E_T > 8$ GeV, irrespective of the isolation of the muon track. Evidently, this analysis is only possible in the case of muons, since they penetrate the calorimetry and have detectable tracks in the outer muon chambers after all other jet debris have been absorbed. After scanning and excluding events previously identified with $W \to \mu\nu$ and $Z^0 \to \mu^+\mu^-$ decays, we are left with 59 events, mostly containing muons embedded in jets. Background due to pion and kaon

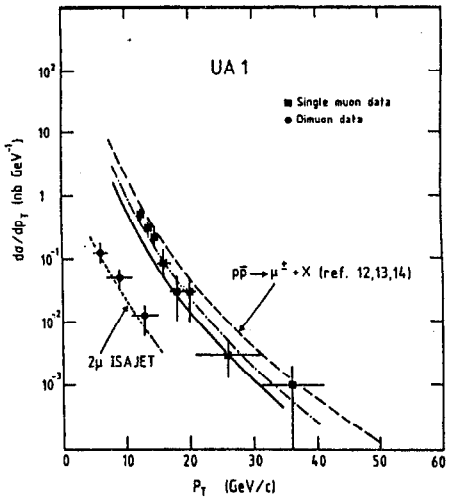

Fig. 20 : Measured inclusive muon p_T spectrum (solid squares) with no isolation cuts. The upper curves are theoretical predictions of the inclusive muon rate from b- and c-quarks: Horgan and Jacob [16] (dashed), Halzen and Scott [17] (dot-dashed), and Kinnunen [18] (solid). Also plotted is the muon p_T spectrum from dimuon events (solid circles, two entries per event). The lower curve (dotted) is a prediction, using ISAJET, [19] of the dimuon rate from b- and c-quark decay assuming a total cross-section consistent with the inclusive single muon rate.

decays has been calculated from the inclusive momentum spectrum of charged tracks and found to be $\leq$10%. The resulting cross-section for muon inclusive production corrected for detection efficiency is shown in Fig. 20. It appears to be in excellent agreement with theoretical calculations [16–19] of large-p_T ($c\bar{c}$) and ($b\bar{b}$) production with subsequent leptonic decay. In order to further verify the associated production nature of the events, we have selected, also inclusively, events with *two* prompt muons, of either equal or opposite signs and $p_T > 5$ GeV/c. The muon transverse momentum spectrum from the resulting 10 events is again in good agreement with the theoretical expectations of ISAJET. [15] QCD calculations of the reactions (1) have been carried out incorporating the requirement that the final state fulfils our selection criteria.[20] The background, mainly from ($b\bar{b}$) states with a final hard parton, amounts to at most 1% of the expected signal from $W \rightarrow t\bar{b}$. Thus, at least within the framework of QCD, the backgrounds due to ($b\bar{b}$) and ($c\bar{c}$) production are negligible.

However, in view of the limited experience with these processes, a model-independent determination of this background is highly desirable. Therefore, a more direct method has been employed, which relies empirically on isolation and topology to differentiate between backgrounds and signal. As in the previous section, this analysis is based on the inclusive muon sample. In order to evaluate the effects of the isolation cut, all particles in a cone $\Delta R \leq 1$ around the muon of $p_T > 12$ GeV/c have been neglected. Events with a clean two-jet topology outside this cone have been selected and carefully scanned. In addition to the known, isolated events, 17 other events have been found in which the jet algorithm finds also a jet inside the $\Delta R \leq 1.0$ cone around the muon. These events have all the properties expected from processes (1), namely: i) the higher E_T jet tends to be back-to-back with the muon in the transverse plane, $\Delta\phi(\mu j_1) \simeq 180°$, and ii) the softer jet is sharply collimated around the incoming beam directions $|\cos\theta^*_{j_2}| \simeq 1$, indicating the gluon bremsstrahlung nature of the softer parton emission. These distributions (shown in Fig. 21a) are completely different from the ones for isolated events (Fig. 21b), which are somewhat broader in $\Delta\phi(\mu j_1)$ and flat in $\cos\theta^*_{j_2}$. The cut, $\Delta\phi(\mu j_1) \leq 155°$, $|\cos\theta^*_{j_2}| < 0.8$ removes all 17 non-isolated events and retains 5/6 of the isolated ones. If the isolated events were also of origin (1), both samples should have the same topology, since isolation depends only on the detailed fragmentation of the 'jet' into the muon and other debris. The probability that the two samples have an identical source is $P = 3 \times 10^{-4}$, equivalent to a 3.6 st. dev. effect.

Further independent evidence of the different origin of the two samples can be gained by comparing the invariant masses $m(\mu\nu_T j_1 j_2)$ of isolated and non-isolated events (Fig. 22a). Whilst the isolated lepton events (both electrons and muons) cluster around the mass of the W, thus supporting the $W \rightarrow t\bar{b}$ hypothesis, the non-isolated muon events are distributed over a broader mass range. Selecting muon events in the mass range $60\ \text{GeV/c}^2 < m(\mu\nu_T jj) < 100\ \text{GeV/c}^2$ and looking at the total energy deposited in a restricted cone $\Delta R \leq 0.4$, we find predominantly isolated events. For these isolated muons, the additional energy deposition in the cone is consistent with the expected random energy deposition from the underlying event as measured from a clean sample of QCD two-jet events (Fig. 22b). Using ISAJET and known fragmentation factors to extrapolate the shape of the background in the region $\Sigma E_T < 2$ GeV, we find an expected background of 0.15 events, in excellent agreement with theoretical QCD predictions. Therefore we conclude that b and c associated processes cannot be the origin of the observed signal.

3.4 Interpretation of the events

We will now proceed to examine the physical origin of the six events with a lepton (muon or electron) and two jets. An example of one of these events is shown in Fig. 23. In Fig. 24 we show the effective mass of the lepton, two jets, and the transverse component of the neutrino. A very sharp peak can be observed at a value corresponding to the W mass, once we have allowed for the small shift and broadening arising from the neglect of the longitudinal component of the neutrino momentum.[21]

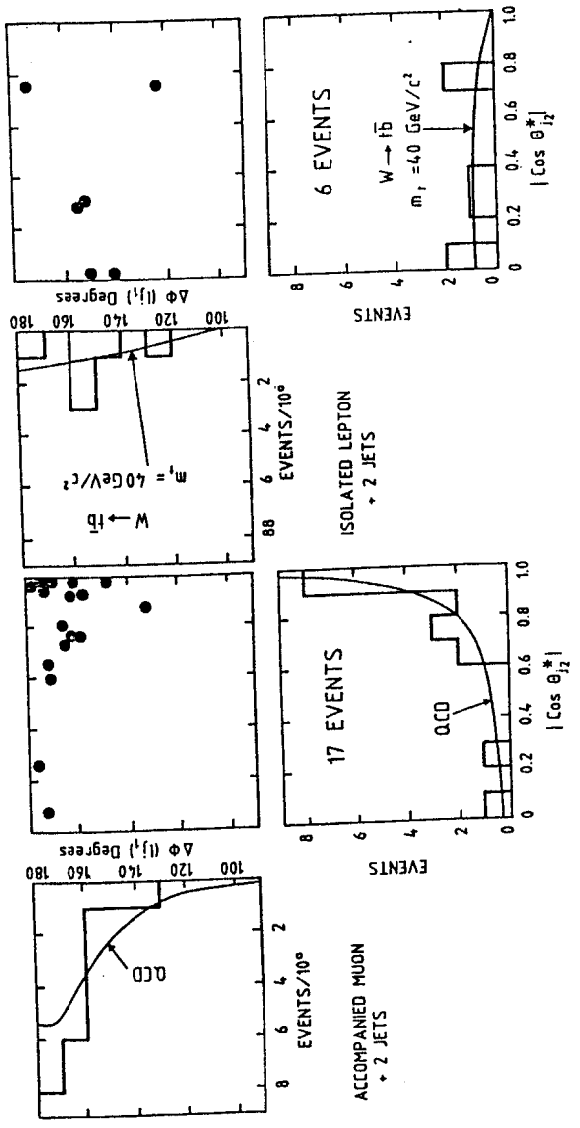

Fig. 21 : Lepton + 2 jet event shape for a) the non-isolated muon sample for which the lowest E_T jet is central ($|\cos\theta^*_{j_2}| < 0.8$), and b) the isolated electron and isolated muon samples. The angle in the transverse plane between the lepton and the highest E_T jet, $\Delta\phi(l_{j_1})$, is shown as a function of $\cos\theta^*_{j_2}$ (see Fig.19). The curves show the expectation [7] for a) QCD background events from process (1), and b) $W \to t\bar{b}$ events with a top-quark mass $m_t = 40\ GeV/c^2$.

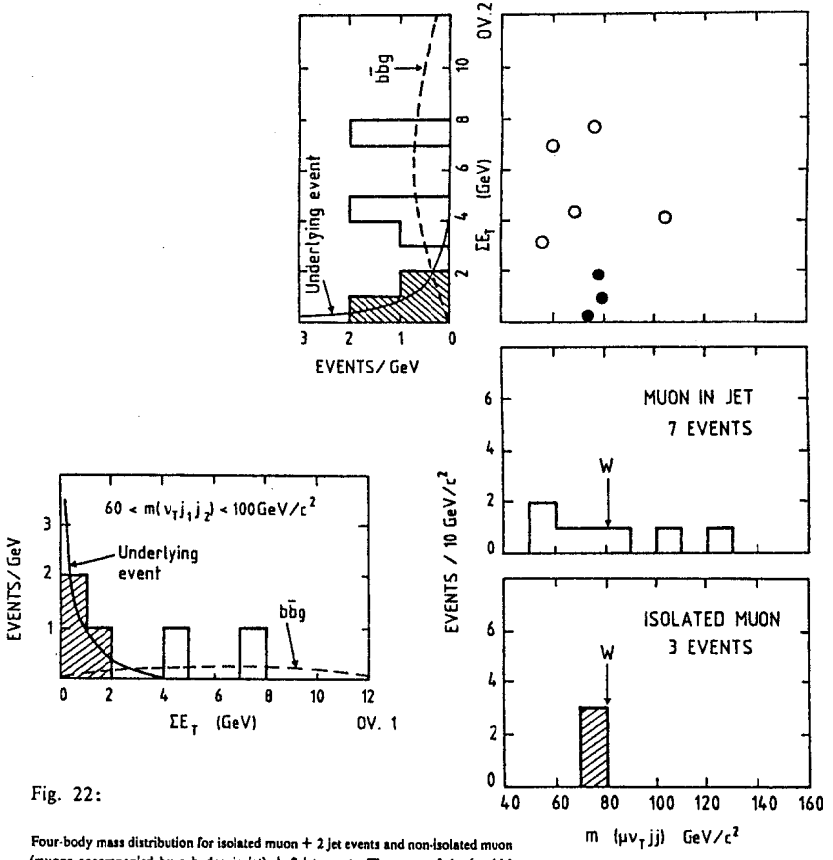

Fig. 22:

Four-body mass distribution for isolated muon + 2 jet events and non-isolated muon (muons accompanied by a hadronic jet) + 2 jet events. The mass of the $(\mu\nu_T j_1 j_2)$ system is plotted as a function of the muon isolation parameter ΣE_T, the additional energy deposited is a cone $\Delta R = 0.4$ around the muon. a) The isolated muon (shaded) events show a peak at the W mass. The distribution for the isolated events agrees with that expected for genuinely isolated muons, the ΣE_T arising from a random contribution from the underlying event (solid curve). The ΣE_T distribution for the non-isolated events agrees with an ISAJET prediction for the background from process (1) (broken curve). b) The ΣE_T distribution is shown for those events lying in the region of the W mass in the $m(\mu\nu_T j_1 j_2)$ distribution. These events are predominantly isolated (solid curve) with only a small contamination from QCD background events (broken curve).

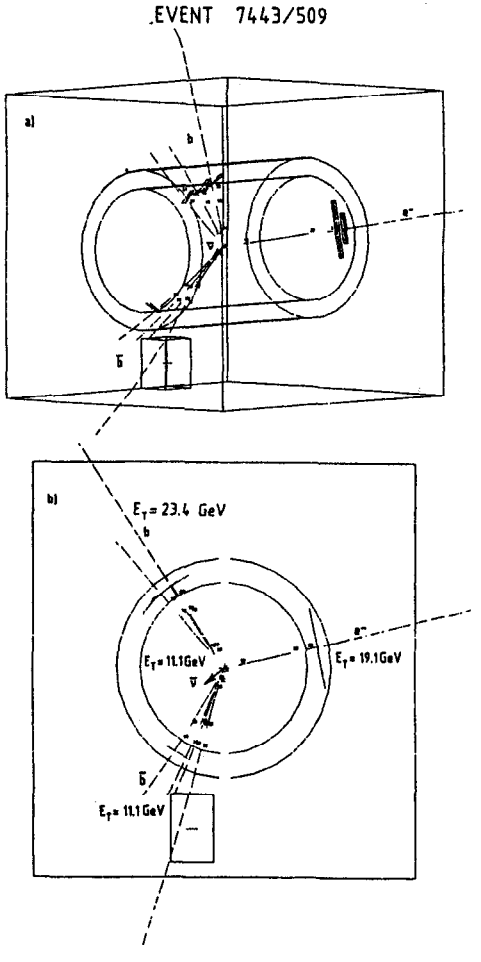

Fig. 23 : Graphic display of calorimeter cells and charged tracks observed in the UA1 detector for event 7443/509, a $W^- \to \bar{t}b$ candidate: a) general view, and b) view looking along the beam direction. The decay products (b, $\bar{b}$, e^- and $\bar{\nu}$) are labelled.

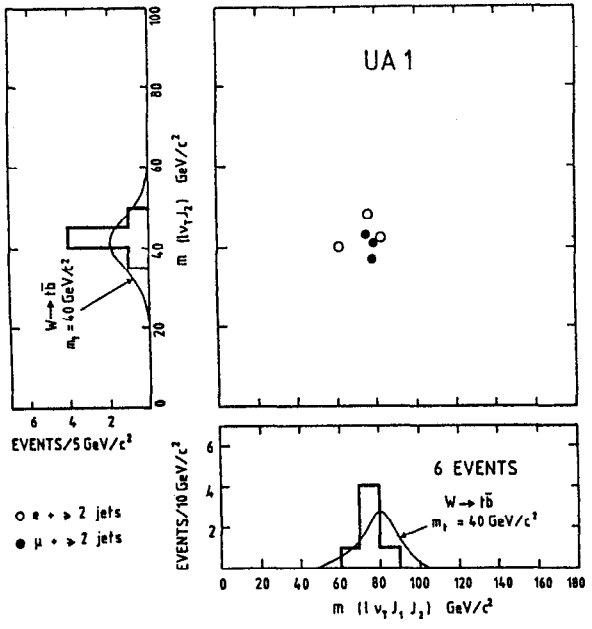

Fig. 24 : Four-body versus three-body mass distribution for the six $W \to t\bar{b}$ candidate events. The effective mass of the lepton, the lower-E_T jet, and of the transverse component of the neutrino is plotted against the mass of the lepton, two-jet, transverse neutrino system. The four-body mass peaks at the W mass. The three-body mass clusters around a common value of $\sim$ 40 GeV/c². The curves show the expected [21] distributions, taking into account the experimental resolution. Allowance should be made for a systematic error arising from uncertainties in the jet reconstruction ($\pm$ 10 GeV/c²).

The reconstruction of invariant masses from jets is a novel technique and it deserves some discussion. Jet finding is done in the calorimeters with the standard UA1 algorithm which associates both electromagnetic and hadronic cells in (η,ϕ) space with $\Delta R = (\Delta\eta^2 + \Delta\phi^2)^{\frac{1}{2}} < 1$. The initiators, which form the core of these jets, must have cells with $E_T \geq 1.5$ GeV. Only cells with $|\eta| < 2.5$ are used for jet finding. Jets are defined with $E_T > 8$ GeV (first jet), whilst other jets within the same event are defined with $E_T > 7$ GeV. Two corrections have to be introduced to derive the

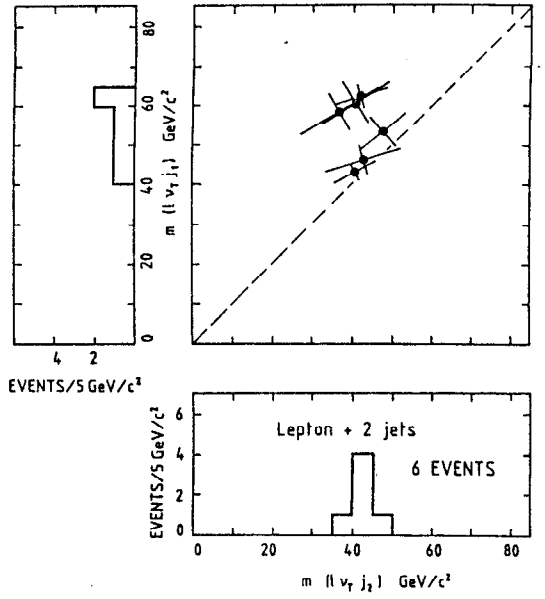

Fig. 25 : The two solutions for the three-body mass distributions $m(\ell\nu_T j)$. The solution using the lower E_T jet, $m(\ell\nu_T j_2)$, gives a distribution consistent with a common value of $\sim$ 40 GeV/c^2. The other solution using the higher E_T jet gives a broader distribution extending to higher masses.

'true' jet energy: i) some of the jet debris can fall outside the cone of acceptance and therefore energy must be added, and ii) some of the uncorrelated low-energy tracks from the underlying event may be added by the jet-finding algorithm and their average contribution must be subtracted. A very complete Monte Carlo calculation has been set up to take into account these effects, starting from the measured fragmentation functions and including the detector properties. Tables of correction factors and of errors have been generated in this way [22] and used to calculate 'true' energies. It can be seen in Fig. 24 that, within these errors, all six events are consistent with a common mass m_W.[23] Therefore, we conclude that we are observing a novel, semileptonic decay of the W particle.

In order to identify the decay mode, we can next evaluate the invariant mass of the lepton, the neutrino, and one of the jets. In Fig. 24, we also show the three-body mass distribution $m(\ell\nu_T j_2)$ obtained by selecting the lower-transverse-energy jet. A sharp peak is observed around 40 GeV/c^2. The other solution, based on the other choice of jet, gives a broader spectrum, extending to higher masses (Fig. 25). For three events, both choices give consistent mass values. For the other three events, we prefer the low-mass solution since i) the high mass corresponds to decays strongly suppressed by phase space, and ii) Monte Carlo simulation shows that, for $W \to t\bar{b}$ events, this is the right choice in the majority of cases. Therefore, we conclude that we have observed a new particle state amongst the debris of the W decays; this state subsequently decays semileptonically. All jets have invariant masses of less than 10 GeV/c^2, which sets an upper limit to the mass of the underlying partons.[24]

The decay hypothesis $W \to t\bar{b}$ with $m_t \simeq 40$ GeV/c^2 describes all kinematical distributions [25] very well, as shown in Fig. 26. The rate of occurrence of the events, the number of $W \to e\nu$ decays, and the Monte Carlo determined detection efficiency can be combined in order to evaluate the top semileptonic branching ratio, which is 0.23 ± 0.09, to be compared [23] with 0.13 for b-quarks and 0.12 for the lighter, charmed quarks.

Finally, we quote a systematic error of ± 10 GeV/c^2 in the mass evaluations. This is primarily due to uncertainties in the reconstruction of jets and the determination of the associated parton four-vectors.

In addition to the six lepton + 2 jet events we have been discussing, there are three lepton + 3 jet events (Table 5). The rate and topology of these events are not inconsistent with the hypothesis of ($t\bar{t}$) associated production. However, owing to the combinatorial problems and the complexity of the topology, the analysis is more difficult and is still in progress.

Table 5

Event parameters for the isolated lepton + 3 jet events

Event	Type	Lepton			ΔE_m	Jet 1			Jet 2			Jet 3		
		E_T	η	ϕ		E_T	ϕ	η	E_T	ϕ	η	E_T	ϕ	η
7700/487	μ^-	21.4 ± 2.6	1.7	−12	2.2 ± 7.0	22.9	−161	1.3	12.0	61	1.8	9.5	31	0.3
5069/192	e^+	15.0 ± 0.7	0.7	−41	26.7 ± 5.7	19.5	−150	−0.7	14.1	32	−0.5	13.0	−149	0.8
6899/804	e^-	18.0 ± 0.8	−0.3	−58	9.7 ± 5.7	16.9	83	0.6	8.8	−121	−0.1	8.5	169	−0.7

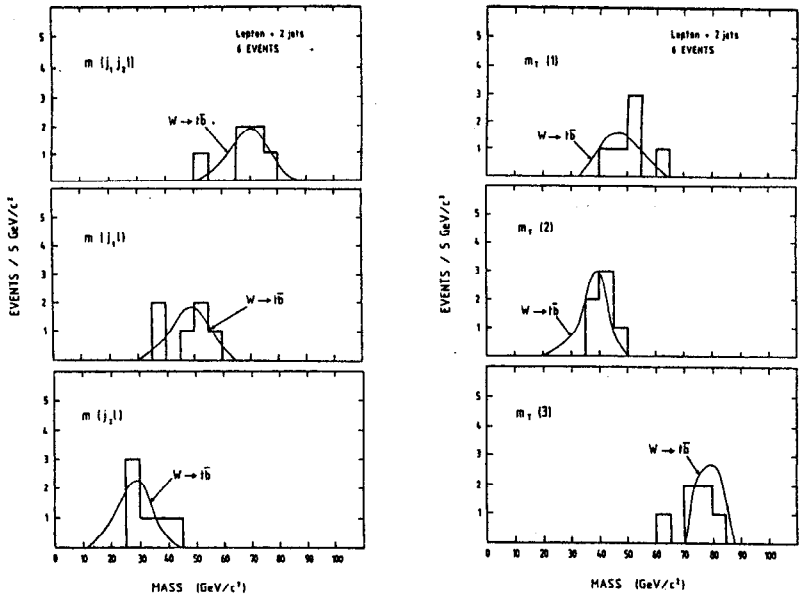

Fig. 26 : Kinematic distributions for the six $W \to t\bar{b}$ candidates, compared with theoretical expectations [25] for a top mass $m_t = 40$ GeV/c^2. a) Mass distributions for i) the lepton two-jet system $m(j_1 j_2 \ell)$; ii) the lepton highest-E_T jet system $m(j_1 \ell)$; and iii) the lepton lowest-E_T jet system $m(j_2 \ell)$. b) Transverse mass distributions defined in Ref. [25]:

i) $m_T(1); m_T^2(1) \equiv m_W^2 + m_b^2 - 2m_W(m_b^2 + \vec{b}_T^2)^{\frac{1}{2}}$, where $\vec{b}_T$ is the transverse momentum of the highest E_T jet;

ii) $m_T(2) \equiv m_T(b\ell,\nu)$, where $m_T^2(c\nu) \equiv (c_T^0 + \nu_T)^2 - (\vec{c}_T + \vec{\nu}_T)^2$ and $c_T^0 = (\vec{c}_T^2 + m_c^2)^{\frac{1}{2}}$;

iii) $m_T(3) \equiv m_t(\bar{b}b\ell;\nu)$.

4. CONCLUSIONS

We observe a clear signal in the channel of an isolated large-transverse-energy lepton plus two or three associated jets. The two-jet signal has an over-all invariant mass clustering around the W mass, indicating a novel decay of the W. The rates and features of the two-jet events do not satisfy the expectations for charm and beauty decay. They are, however, consistent with the process $W \to t\bar{b}$, where t is the sixth 'top' quark of the Cabibbo current. If this is indeed the case, then the mass of the top is bounded between 30 and 50 GeV/c^2. We stress that the present uncertainty in the $(\ell\nu_T j_2)$ mass is due to the determination of the jet energies, and that more statistics are needed to confirm these conclusions and the true nature of the effect observed.

REFERENCES AND FOOTNOTES

[1] Minimum bias events are triggered by the presence of one or more charged tracks in each of two large hodoscopes surrounding the beam line. We trigger on about 2/3 of the inelastic cross-section. For a description of the detector, see A. Astbury et al., CERN/SPSC/78-06 (1978).

[2] For details of the W event selection, see G. Arnison et al., Phys. Lett. 122B, 103 (1983); G. Arnison et al., Phys. Lett. 129B, 115 (1984).

[3] G. Arnison et al., Phys. Lett. 139B, 115 (1984).

[4] For example, for gluino pair production with each gluino decaying into quark, antiquark, and photino (with the photino stable), our event rate places a lower limit on the gluino mass of about 40 GeV. See J. Ellis and H. Kowalski, CERN Ref. TH.3843 (1984).

[5] G. Arnison et al., Phys. Lett. 122B (1983) 103.
G. Arnison et al., Phys. Lett. 129B (1983) 273.

[6] G. Arnison et al., Phys. Lett. 134B (1984) 469.

[7] UA1 Collaboration, "Hadronic Jet Activity Associated with Intermediate Vector Boson Production at the SPS Collider," presented by S. Geer at the 19th Rencontre de Moriond, La Plagne, 1984.

[8] TASSO Collaboration, M. Althoff et al., Phys. Lett. 138B (1984) 441.
S. Yamada, Proc. 1983 Intern. Symp. on Lepton and Photon Interactions at High Energies (Cornell, 1983); and DESY report 83-100 (1983).
Mark J Collaboration, B. Adeva et al., Phys. Rep. 109 (1984) 1.
S.L. Wu, Phys. Rep. 107 (1984) 1.

[9] G. Arnison et al., Phys. Lett. 139B (1984) 115.
The scalar missing energy ΔE_m is defined as the apparent momentum imbalance in the transverse plane, obtained by adding energy depositions vectorially in all calorimeter cells. Since the calorimetry covers essentially a 4π solid angle, this quantity reflects the transverse component of the momentum of the emitted neutrino(s).

[10] The invariant mass m_t reflects the 'bare' quark mass. Small changes are expected for physical top particles, in which the top quark is bound to 'ordinary,' much lighter quarks. Within the present accuracy, this effect can be neglected.

[11] M. Barranco Luque et al., Nucl. Instrum. Methods 176 (1980) 75.
M. Calvetti et al., Nucl. Instrum. Methods 176 (1980) 255.
M. Calvetti et al., IEEE Trans. Nucl. Sci. NS-30 (1983) 71.
M. Corden et al., Phys. Scr. 25 (1982) 5 and 11.
K. Eggert et al., Nucl. Instrum. Methods 176 (1980) 217.
The UA1 Collaboration is preparing a comprehensive report on the detector, to be published in Nucl. Instrum. Methods (NIM).

[12] M. Della Negra et al., **Expected Rate of Background to the Electron Sample from Conversions**, CERN UA1-TN/84-76 (1984).

[13] E. Eisenhandler et al., CERN UA1-TN/84-64 (1984).
χ^2_R measures the goodness of fit to the electron hypothesis. This parameter has been developed from a study of electron test-beam data making full use of the longitudinal profile of the shower measured in the four samplings of the electromagnetic calorimeter, and taking into account the electron energy and angle of incidence.

[14] This effect is well understood according to QCD since the third jet is mostly due to gluon bremsstrahlung from the incoming partons. Experimental verification of this rather general property has been observed at the collider both for QCD jets and for W + jet events. For more details, see Ref. 7.

[15] M. Della Negra et al., **Background Study to e^+ Jet Events**, CERN UA1-TN/84-77 (1984).

[16] R. Horgan and M. Jacob, Nucl. Phys. B238 (1984) 221.

[17] F. Halzen and D.M. Scott, Phys. Lett. 129B (1983) 341.

[18] R. Kinnunen, private communication, and Ph. D. thesis, Univ. Helsinki, 1984 (to be published).

[19] F.E. Paige and S.D. Protopopescu, ISAJET program, BNL 29777 (1981).
B. Humpert, Phys. Lett. 85B (1979) 293.

[20] I. Schmitt, L.M. Sehgal, H. Thode and P.M. Zerwas, **Stimulation of t-quark Production by a Hard Three-parton Final State in $p\bar{p}$ Collisions**, Univ. Aachen preprint PITHA 83/26 (1983).
L.M. Sehgal and P.M. Zerwas, Univ. Aachen preprint PITHA 83/10 (1983), Nucl. Phys. B, in press.
V. Barger, A.D. Martin and R.J.N. Phillips, Phys. Lett. 125B (1983) 343; Phys. Rev. D28 (1983) 145.
R.M. Godbole, S. Pakvasa and D.P. Roy, Phys. Rev. Lett. 50 (1983) 1539.
F. Halzen and D.M. Scott, Phys. Lett. 129B (1983) 341.
K. Hagiwara and W.F. Long, Madison report MAD/PH/117 (1983).
R. Horgan and M. Jacob, CERN preprint Ref. TH.3682 (1983).
J.H. Kühn, Fermilab preprint PUB-83/79-THY (1983).
V. Barger, H. Baer, A.D. Martin and R.J.N. Phillips, Madison report MAD/PH/133 (1983).
R. Odorico, CERN preprint Ref. TH.3678 (1983).

[21] R. Kinnunen, see Ref. [18].

[22] M. Della Negra et al., CERN UA1-TN/84-43 (1984).
M. Della Negra and P. Ghez, CERN UA1-TN/84-15 (1984).
Note that ISAJET [19] gives systematically different results by as much as 10–20% on the jet energies.

[23] Particle Data Group, **Review of Particle Properties**, Rev. Mod. Phys. 56 (1984).

[24] This strongly suggests a decay into u, d, c, b quarks, since the quark spectrum below 10 GeV/c^2 is well known and fully explored by e^+e^- experiments.

[25] V. Barger et al., CERN preprint Ref. TH.3972 (1984), submitted to Physics Letters.